

## Supporting Information

### Periphery Hindered Strategy of Dopant and Sensitizer for Solution-Processed Red TSF-OLEDs with High Color Purity

Guimin Zhao, Renyin Zhou, Guanghao Zhang, Haowen Chen, Daiyu Ma, Wenwen Tian, Wei Jiang\*, Yueming Sun

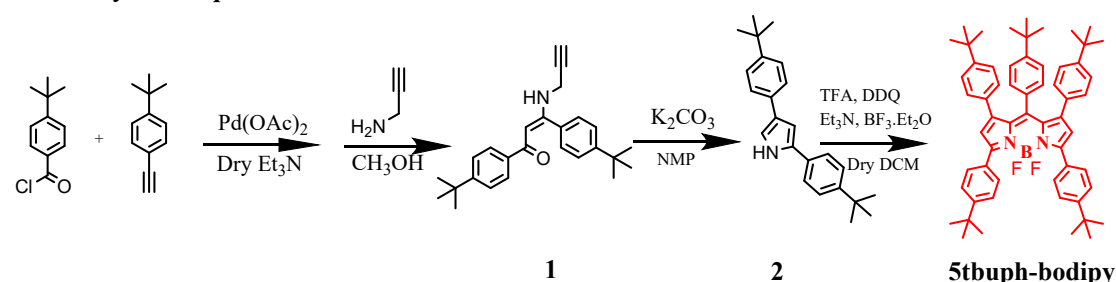
Jiangsu Province Hi-Tech Key Laboratory for Bio-Medical Research, Jiangsu Engineering Laboratory of Smart Carbon-Rich Materials and Device, School of Chemistry and Chemical Engineering, Southeast University, Nanjing, Jiangsu, 211189, China.

\*Corresponding author:

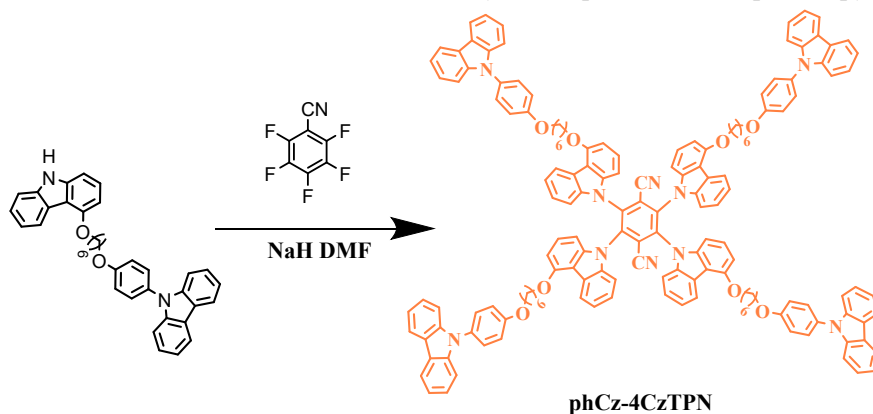
E-mail addresses: jiangw@seu.edu.cn (W. Jiang).

## 1. Experimental Section

### 1.1 The synthesis procedure



Scheme S1. The molecular structure and synthetic process of 5tbuph-bodipy.



Scheme S2. The molecular structure and synthetic process of phCz-4CzTPN.

Unless otherwise indicated, all materials and solvents were obtained from commercial suppliers and used without further purification. 2,3,5,6-tetrafluoroterephthalonitrile was purchased from Energy Chemical. 4-((6-(4-(9H-carbazol-9-yl)phenoxy)hexyl)oxy)-9H-carbazole was prepared according

to the literature.

**The synthesis of (E)-1,3-bis(4-(tert-butyl)phenyl)-3-(prop-2-yn-1-ylamino)prop-2-en-1-one (1)**

A mixture of 4-tert-butylbenzoyl chloride (12.43 g, 63.2 mmol), 4-tert-Butylphenylacetylene (10 g, 63.2 mmol), dry Et<sub>3</sub>N (200 mL) and Pd(OAc)<sub>2</sub> (0.71 g, 3.16 mmol) was stirred at room temperature for 4 h in nitrogen until complete consumption of starting material as monitored by TLC. If the solubility is not good, a small amount of THF can be added. After completion, the reaction mixture was extracted with ethyl acetate. The organic layer was washed with water to dissolve the amine hydrochloride formed. The organic layer was then separated, dried over MgSO<sub>4</sub>, and concentrated under vacuum. After dried overnight under vacuum conditions, the crude product was directly used in the next reaction.

A mixture of the crude product, 2-propynylamine (3.83g, 69.54 mmol), and CH<sub>3</sub>OH (150 mL) was stirred at 65 °C under air overnight. After 2-propynylamine was exhausted completely (monitored by TLC), the solvent was evaporated and the crude product was purified by column chromatography on silica gel (petroleum ether /dichloromethane = 3:1, v/v) to give (E)-1,3-bis(4-(tert-butyl)phenyl)-3-(prop-2-yn-1-ylamino)prop-2-en-1-one as a white solid (13.2 g, 35.4 mmol). Yield: 56%. <sup>1</sup>H NMR (600 MHz, CDCl<sub>3</sub>): δ 11.31 (s, 1H), 7.84-7.83 (m, 2H), 7.49-7.47 (m, 2H), 7.44-7.41 (m, 4H), 5.84 (s, 1H), 3.98-3.96 (m, 2H), 2.31 (s, 1H), 1.36 (s, 9H), 1.36 (s, 9H).

**The synthesis of 2,4-bis(4-(tert-butyl)phenyl)-1H-pyrrole (2)**

A mixture of **1** (7.46 g, 20 mmol), K<sub>2</sub>CO<sub>3</sub> (2.76 g, 20 mmol), and NMP (100 mL) was stirred at 90 °C under air atmosphere for 12 h. After cooling to room temperature, the mixture was extracted with CH<sub>2</sub>Cl<sub>2</sub>, and the organic layer was washed with water and then dried over MgSO<sub>4</sub> and concentrated. The crude product was purified by column chromatography on silica gel (petroleum ether /dichloromethane = 4:1, v/v) to give 2,4-bis(4-(tert-butyl)phenyl)-1H-pyrrole (3.31 g, 10 mmol) as a white solid. Yield: 50%. <sup>1</sup>H NMR (600 MHz, CDCl<sub>3</sub>): δ 8.39 (s, 1H), 7.50 (m, 2H), 7.45-7.42 (m, 2H), 7.40-7.38 (m, 4H), 7.09 (s, 1H), 6.76 (s, 1H), 1.34 (s, 18H).

**The synthesis of 1,3,7,9,10-pentakis(4-(tert-butyl)phenyl)-5,5-difluoro-5H-4H,5H-dipyrrolo[1,2-c:2',1'-f][1,3,2]diazaborinine (5tbuph-bodipy)**

The intermediate 2,4-bis(4-(tert-butyl)phenyl)-1H-pyrrole (1.15 g, 3.47 mmol) was completely dissolved in a solution of dry dichloromethane (25 mL), and 4-tert-butylbenzaldehyde (0.26 g, 1.58 mmol) was added. The mixture was stirred under nitrogen atmosphere for 12 h after the BF<sub>3</sub>•Et<sub>2</sub>O (107 μL, 1.58 mmol) was added. Then, 2,3-dichloro-5,6-dicyano-1,4-benzoquinone (DDQ) (0.72 g, 3.16 mmol) was added into the solution to continue for 4 hours. After the reaction, the organic layer was washed with saturated sodium bicarbonate aqueous solution, then extracted with water, and the blended organic layer was concentrated and dried.

Then, the crude material was dissolved in dry dichloromethane (25 mL), and dried triethylamine (4.68 mmol) and dried boron trifluoride ethyl ether (9.36 mmol) were added, and then was heated to reflux and reacted for 24 h under the protection of nitrogen. After completion, the organic phase was washed with saturated sodium bicarbonate aqueous solution, and then extracted with water. The organic phase was dried and further separated and purified. Finally, the crude product was isolated by column chromatography on silica gel (petroleum ether /dichloromethane = 3:1, v/v) to give 1,3,7,9,10-pentakis(4-(tert-butyl)phenyl)-5,5-difluoro-5H-4H,5H-dipyrrolo[1,2-c:2',1'-f][1,3,2]diazaborinine (0.2 g, 0.23 mmol) as a violet black solid. Yield: 15%. <sup>1</sup>H NMR (600 MHz, CDCl<sub>3</sub>): δ 7.84-7.83 (m, 4H), 7.44-7.45 (m, 4H), 6.97-6.96 (m, 2H), 6.92-6.91 (m, 4H), 6.71-6.70 (m, 4H), 6.60-6.59 (d, 2H), 6.50 (s, 2H), 1.35 (s, 18H), 1.19 (s, 18H), 1.06 (s, 9H). <sup>13</sup>C NMR (150

MHz, CDCl<sub>3</sub>):  $\delta$  = 156.49, 152.35, 148.84, 147.72, 133.37, 132.04, 130.88, 129.88, 129.26, 129.24, 128.81, 128.33, 125.34, 125.21, 124.44, 124.19, 123.48, 38.75, 34.79, 34.32, 34.24, 31.33, 31.26, 31.24, 31.09, 30.38, 28.94, 23.79, 22.95, 14.05, 10.97. MS (MALDI-TOF) [m/z]: [M]<sup>+</sup> calcd for C<sub>59</sub>H<sub>67</sub>BF<sub>2</sub>N<sub>2</sub>, 852.54; found, 853.543. Elemental analysis: calcd for C<sub>59</sub>H<sub>67</sub>BF<sub>2</sub>N<sub>2</sub>: C 83.08, H 7.92, N 3.28; found: C 83.22, H 7.97, N 3.20.

### **The synthesis of 2,3,5,6-tetrakis(4-((6-(4-(9H-carbazol-9-yl)phenoxy)hexyl)oxy)-9H-carbazol-9-yl)terephthalonitrile (phCz-4CzTPN)**

Under nitrogen atmosphere, 4-((6-(4-(9H-carbazol-9-yl)phenoxy)hexyl)oxy)-9H-carbazole (1 g, 1.9 mmol) in anhydrous THF (40 ml) was added dropwise into an anhydrous THF (20 ml) solution containing NaH (0.12 g, 5 mmol) for 15 min and stirred for 3 h. Then, 2,3,5,6-tetrafluoroterephthalonitrile (0.065 g, 0.325 mmol) in anhydrous THF (20 ml) was added dropwise for 15 min. The solution was stirred for 24 h at room temperature. After that, 250 mL water was added into the solution and the mixture was extracted with CH<sub>2</sub>Cl<sub>2</sub> for three times. The combine organic layer was dried with anhydrous MgSO<sub>4</sub> and the solvent was removed under vacuum. The precipitate was purified by column chromatography on silica gel, resulted in the bright orange-red product (0.58 g, 80%). <sup>1</sup>H NMR (600 MHz, CDCl<sub>3</sub>):  $\delta$  8.16-8.11 (dd, J=17.5 Hz, 8.1 Hz, 7H), 8.09-8.03 (dt, J=15.4 Hz, 8.8 Hz, 4H), 7.42-7.38 (dd, J=14.1Hz, 7.9 Hz, 15H), 7.33-7.32 (d, J=7.8 Hz, 8H), 7.29-7.28 (d, J=7.7 Hz, 10H), 7.23-7.20 (m, 5H), 7.16-7.12 (dd, J=16.9 Hz, 8.6 Hz, 6H), 7.09-7.05 (dd, J=13.4 Hz, 7.1 Hz, 12H), 7.02-7.01 (d, J=5.8 Hz, 3H), 6.96-6.93 (m, 2H), 6.89-6.87 (m, 4H), 4.13-4.11 (m, 8H), 4.04-4.02 (t, J=6.3 Hz, 8H), 1.95-1.88 (dd, J=25.5 Hz, 18.8 Hz, 16H), 1.64 (s, 16H). <sup>13</sup>C NMR (150 MHz, CDCl<sub>3</sub>):  $\delta$  = 158.38, 155.55, 141.37, 140.25, 137.97, 130.07, 128.49, 126.89, 125.81, 124.82, 123.95, 123.27, 123.08, 122.81, 121.76, 120.22, 119.60, 115.56, 113.80, 111.69, 109.71, 108.97, 103.85, 103.76, 102.30, 68.12, 67.92, 29.24, 29.20, 26.02, 25.88. MS (MALDI-TOF) [m/z]: [M]<sup>+</sup> calcd for C<sub>152</sub>H<sub>124</sub>N<sub>10</sub>O<sub>8</sub>, 2218.73; found, 2220.674. Elemental analysis: calcd for C<sub>152</sub>H<sub>124</sub>N<sub>10</sub>O<sub>8</sub>: C 82.28, H 5.63, N 6.31; found: C 82.26, H 5.67, N 6.29.

### **1.2 Materials and measurements**

All compounds are commercial from Chemical Company Ltd. and used in the reaction directly. All reactions were carried out under N<sub>2</sub> atmosphere. <sup>1</sup>H NMR and <sup>13</sup>C NMR spectra were acquired using a Bruker Dex-600/150 NMR instrument using CDCl<sub>3</sub> as a solvent. Mass spectra (MS) were recorded on by matrix assisted laser desorption-ionization time-of-flight mass spectrometry (MALDI-TOF-MS) using a BRUKER DALTONICS instrument, with  $\alpha$ -cyano-hydroxycinnamic acid as a matrix. Elemental analysis was determined by an Elementar Vario EL CHN elemental analyzer. UV-vis absorption spectra were recorded using a SHIMADZU UV-2600 spectrophotometer. Steady-state photoluminescence (PL) spectra were obtained with a HORIBA FLUOROMAX-4 spectrophotometer at room temperature. The transient PL decay was obtained by EDIBURGH FLS-1000 instruments. The low-temperature phosphorescence (PH) spectra were recorded on F-7000 FL spectrophotometer after delayed 100  $\mu$ s under liquid nitrogen. The solid PL quantum efficiencies were measured using an integrating sphere under nitrogen at room temperature. Thermogravimetric analysis (TGA) and differential scanning calorimetry (DSC) curves were carried out with a Netzsch simultaneous thermal analyzer system (STA 409 PC) from 20 °C to 800 °C and DSC 2910 modulated calorimeter from 20 °C to 200 °C at a 10°C/min heating rate under N<sub>2</sub> atmosphere. Cyclic voltammetry measurements were performed using a CHI750C voltammetric analyzer. Electrochemical property was evaluated by cyclic voltammetry with three typical electrodes in dry CH<sub>2</sub>Cl<sub>2</sub> solution (10<sup>-3</sup> M) (oxidation process) with a rate of 100 mV/s. The CV system employed

Bu4NPF6 as electrolyte. Platinum disk is used as the working electrode, platinum wire is regarded as the counter electrode and silver wire is used as the reference electrode. Ferrocenium/ferrocene (Fc/Fc<sup>+</sup>) was used as the external standard compound.

### 1.3 Computation Method

All calculations were conducted using the Gaussian 09 program. The molecular orbitals were visualized using Gaussview 5.0. The geometries were optimized at the B3LYP/6-31G(d) level. The transition energy and oscillator strength were calculated with TD-DFT method at the B3LYP/6-31G(d) level.

### 1.4 OLED Device Fabrication

OLED devices were fabricated using a clean glass substrate coated with an ITO layer (150 nm) as the anode, with a sheet resistance of 15  $\Omega$  cm<sup>-2</sup> and an active pattern size of 2 × 2 mm<sup>2</sup>. Before device fabrication, the glass substrates were sequentially cleaned in an ultrasonic bath with deionized water, acetone and ethanol for three times, and then the ITO substrate was treated with UV-ozone for 30 minutes. The OLED configuration was as follows: ITO (150 nm)/PEDOT:PSS (50 nm)/EML(40 nm)/TPBi (40 nm)/Cs<sub>2</sub>CO<sub>3</sub> (2 nm)/Al (100 nm), where PEDOT:PSS and Cs<sub>2</sub>CO<sub>3</sub> acted as the hole and electron injection layers, respectively. The TPBi and Al functioned as the electron transport layers and the cathode, respectively. The PEDOT:PSS was directly spin-coated on an ITO plate and annealed at 150 °C for 10 min. The EML was dissolved in 1, 2-dichloroethane (10 mg mL<sup>-1</sup>), then spin-coated and annealed at 80 °C for 10 min under nitrogen atmosphere. Then, the substrates were moved into a vacuum chamber to deposit TPBi, Cs<sub>2</sub>CO<sub>3</sub>, and Al sequentially using a thermal evaporator. The current density–voltage–luminance characteristics, current efficiency and power efficiency were tested using a Keithley 2636A Sourcemeter coupled with Si-potodiodes calibrated with PR655. The EL spectra were collected with a Photo-Research PR655 SpectraScan. All the characterizations were performed at room temperature in ambient condition without encapsulation. External quantum efficiencies of the devices were calculated assuming a Lambertian emission distribution.

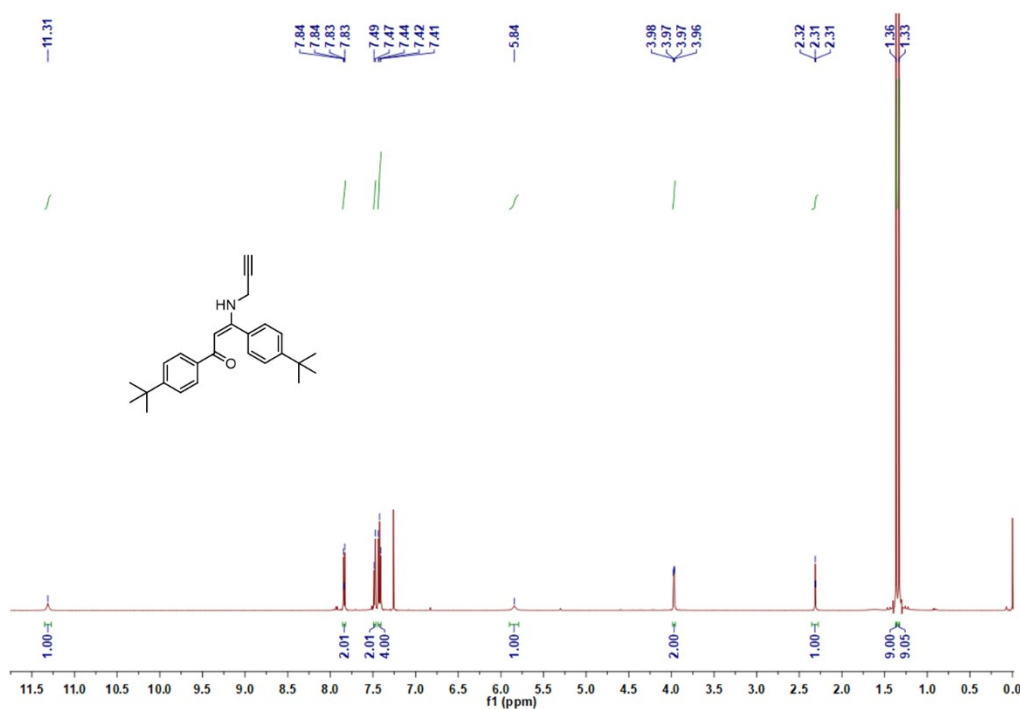


Figure S1.  $^1\text{H}$  NMR spectrum of 1.

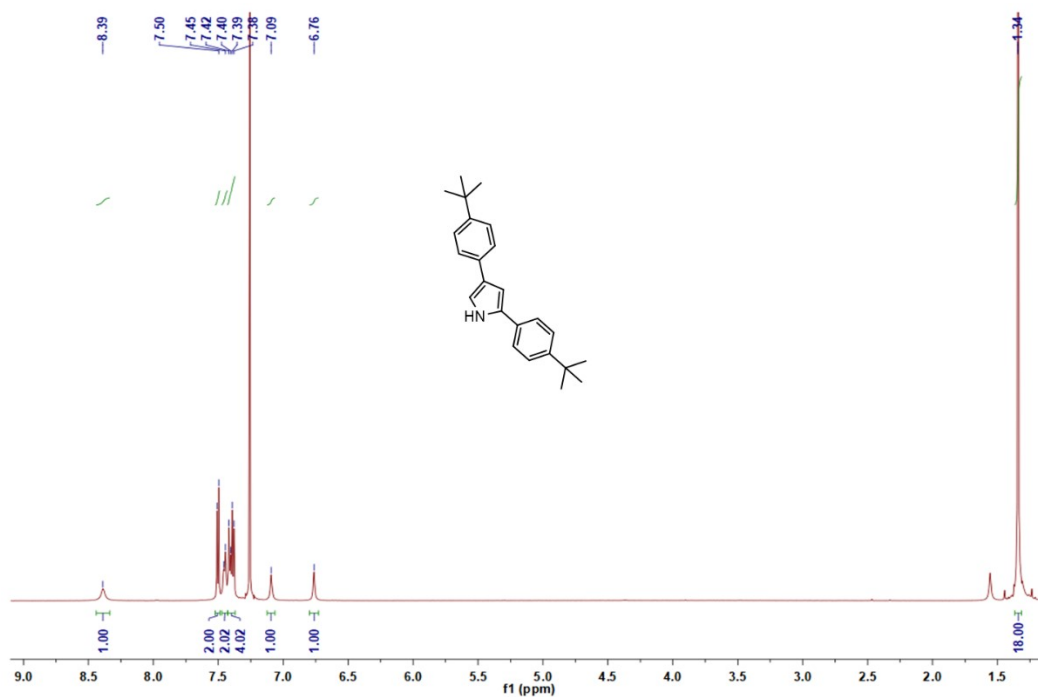


Figure S2.  $^1\text{H}$  NMR spectrum of 2.

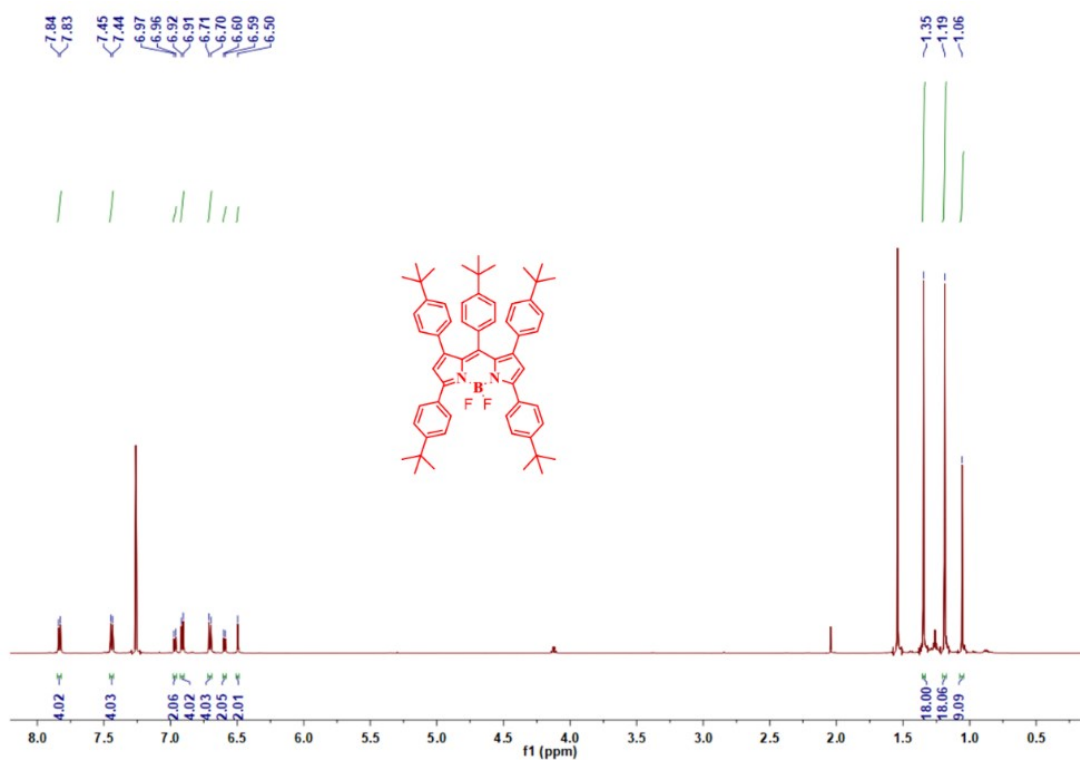


Figure S3.  $^1\text{H}$  NMR spectrum of 5tbuph-bodipy.

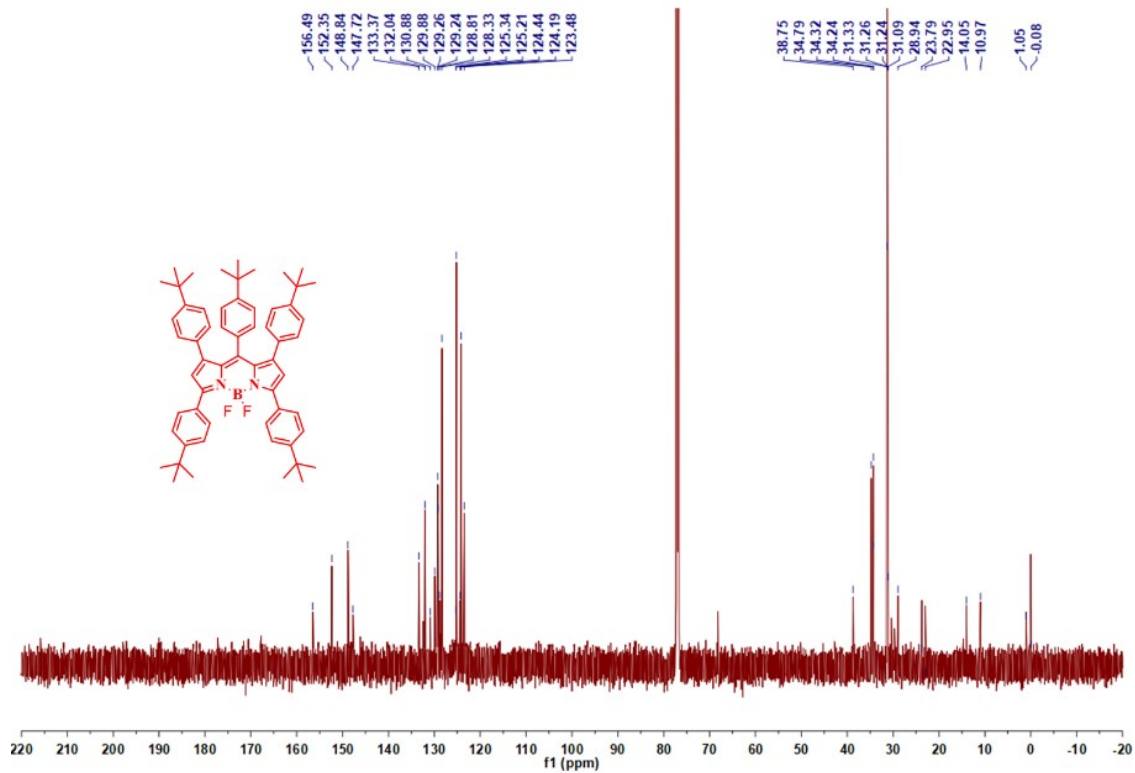


Figure S4.  $^{13}\text{C}$  NMR spectrum of 5tbuph-bodipy.

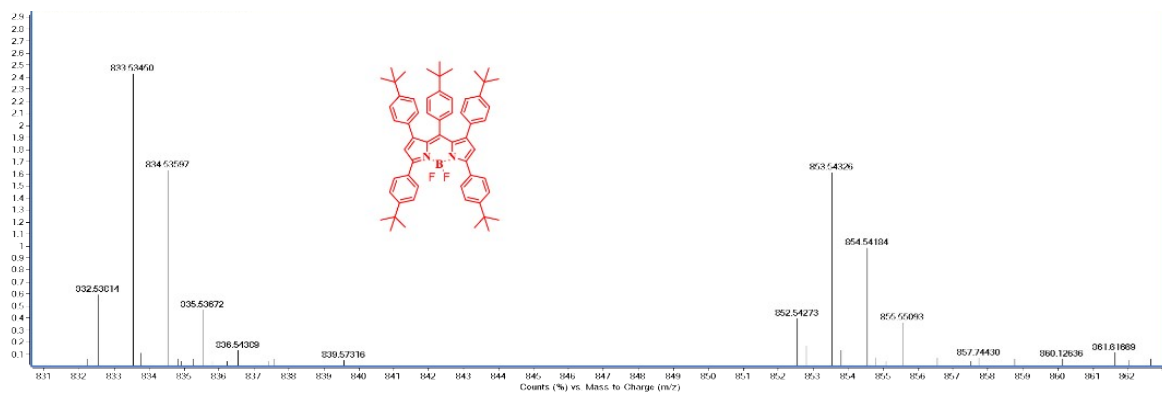


Figure S5. Mass spectrum of 5tbuph-bodipy.

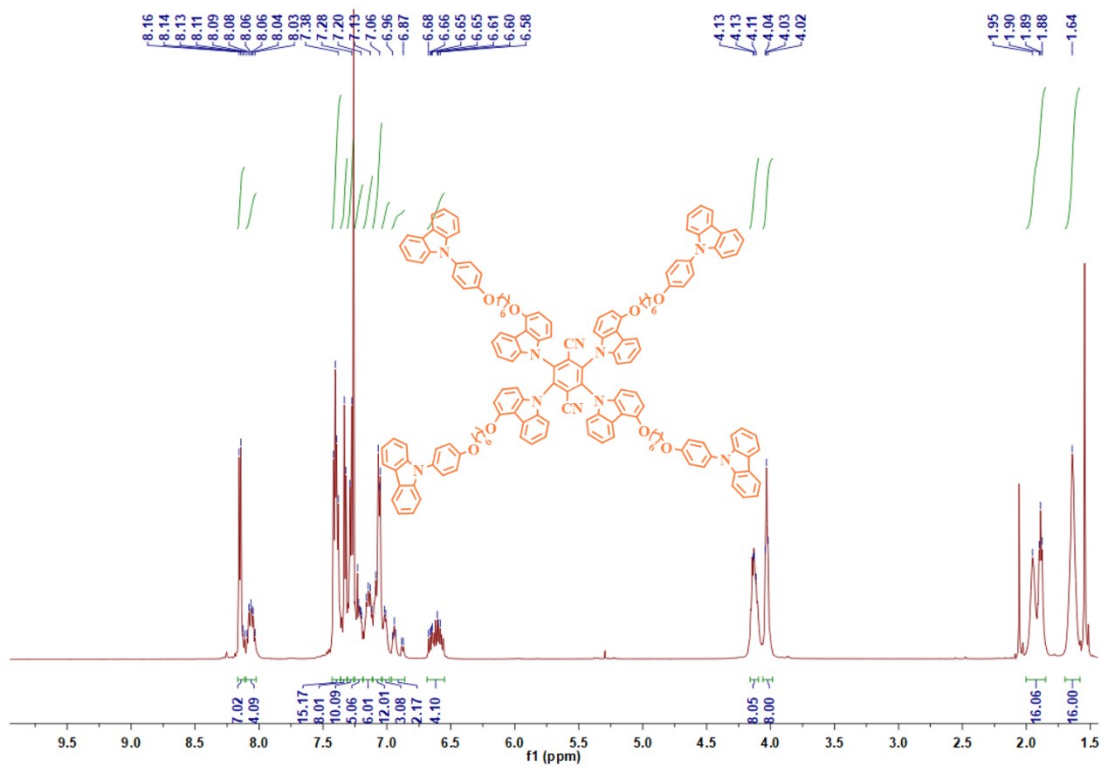


Figure S6.  $^1\text{H}$  NMR spectrum of phCz-4CzTPN.

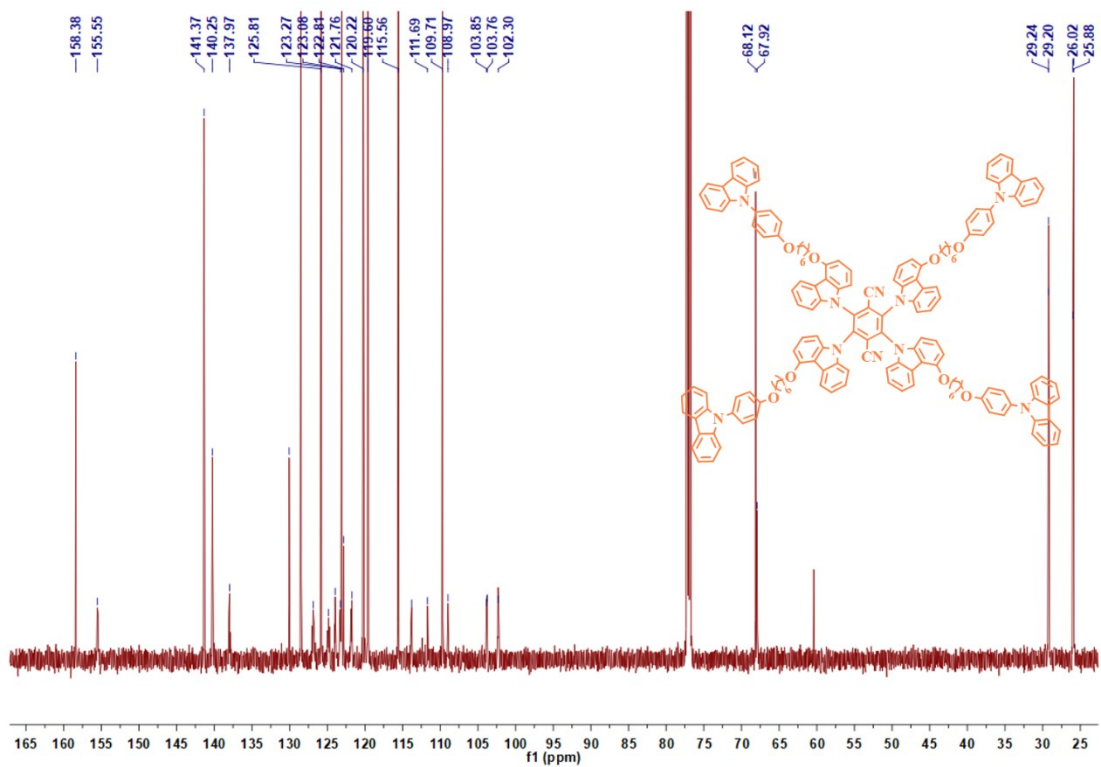


Figure S7.  $^{13}\text{C}$  NMR spectrum of phCz-4CzTPN.

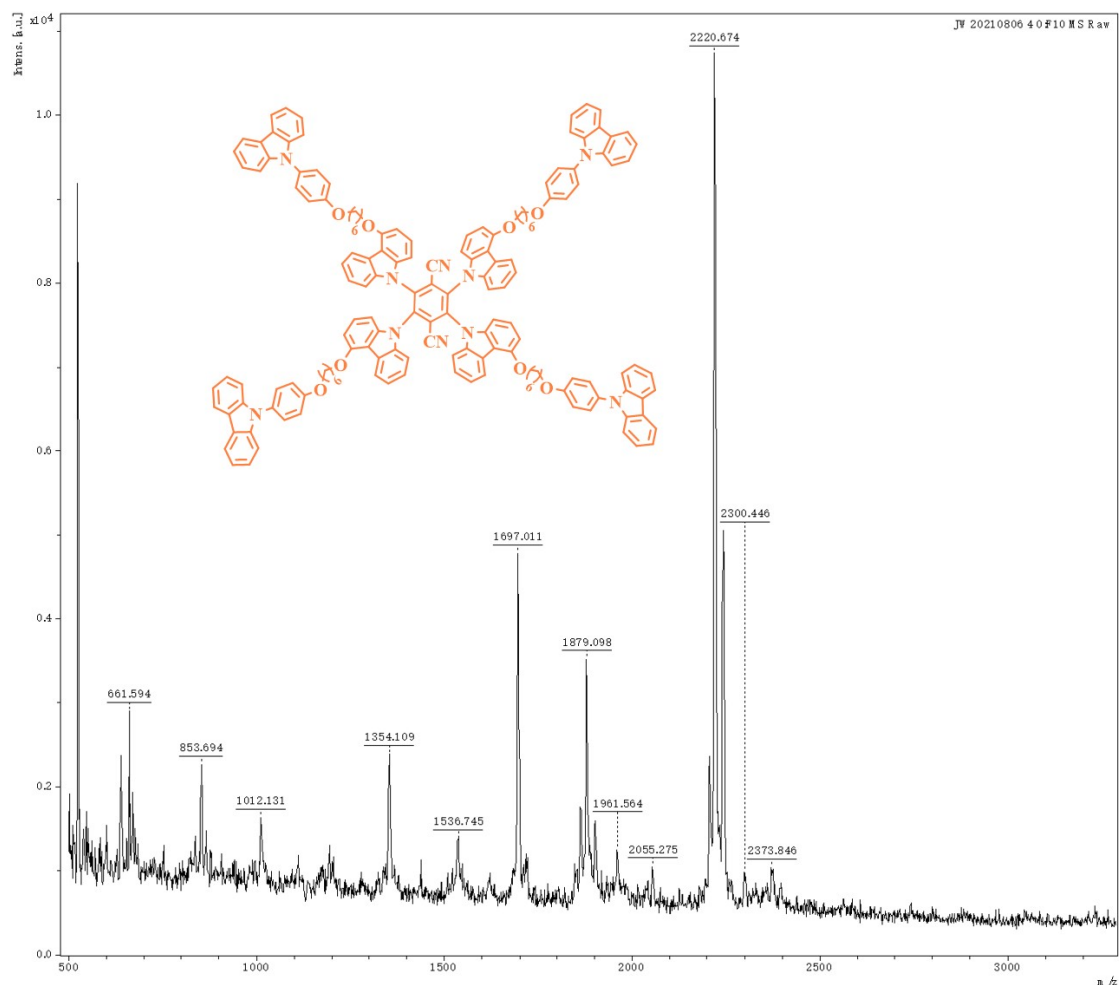


Figure S8. Mass spectrum of phCz-4CzTPN.

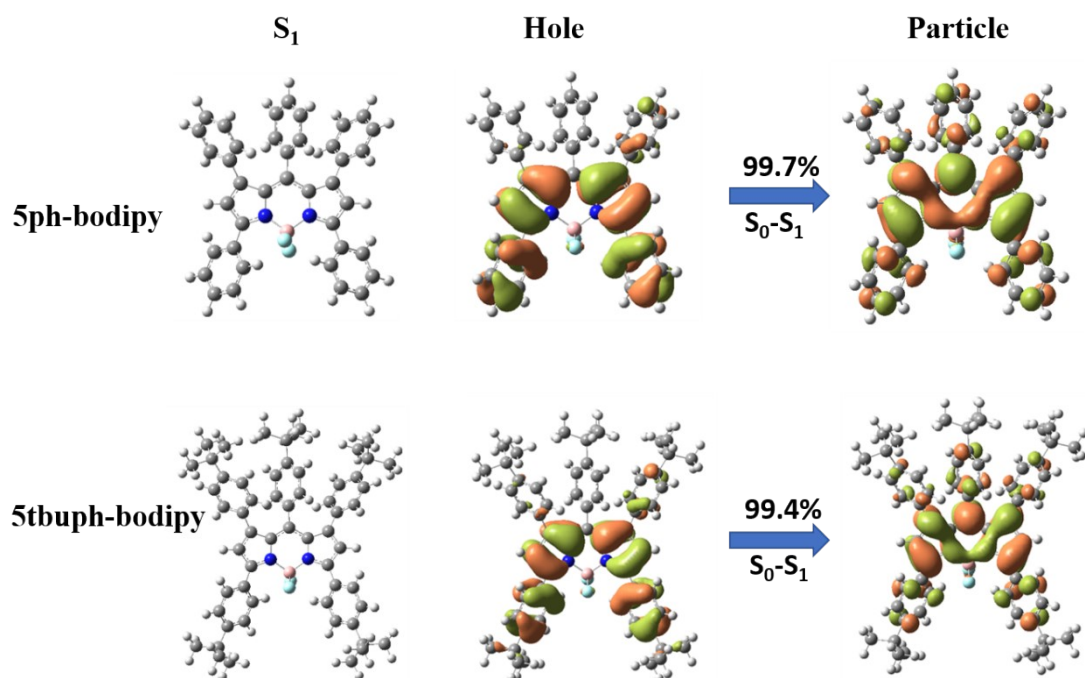


Figure S9. The optimized molecular configuration and the natural transition orbitals (NTOs) distribution of  $S_1$  state for 5ph-bodipy and 5tbuph-bodipy.

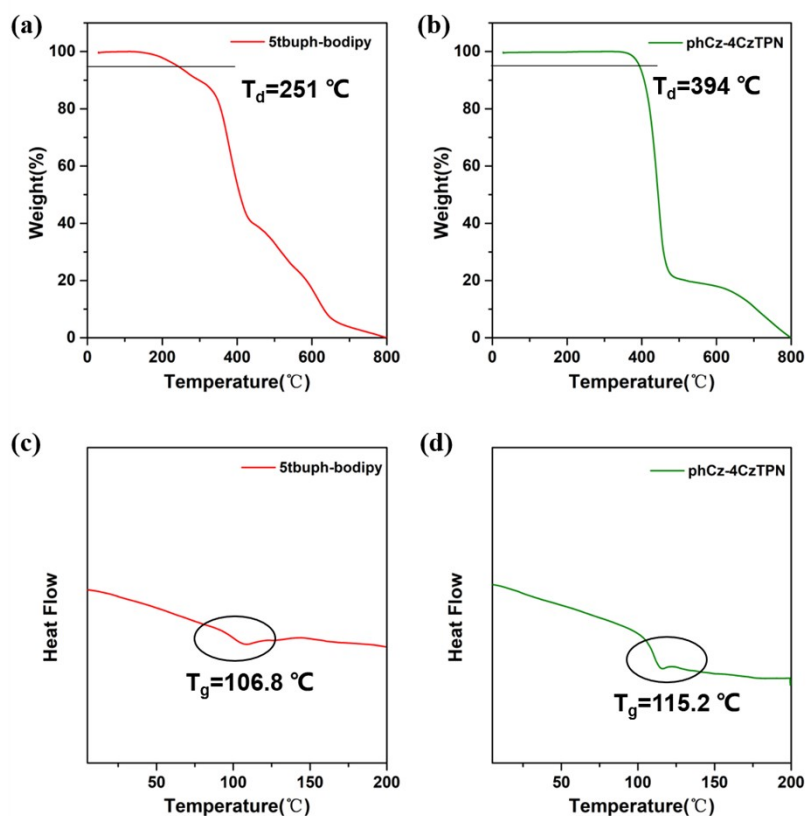


Figure S10. The decomposition temperatures and glass-transition temperatures of 5tbuph-bodipy and phCz-4CzTPN at a heating rate of  $10\text{ °C min}^{-1}$  under a nitrogen atmosphere.

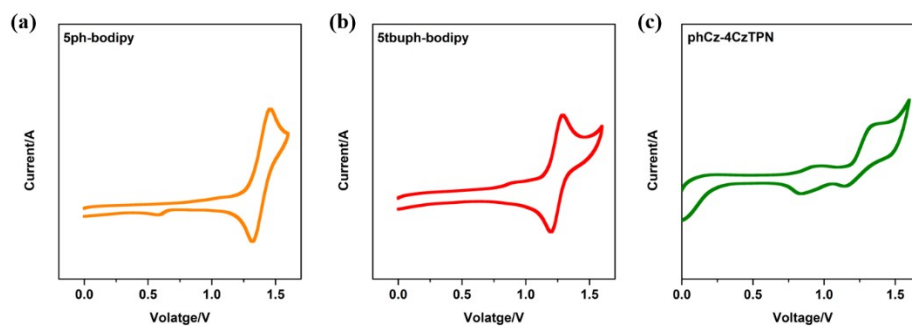


Figure S11. The cyclic voltammetry of 5ph-bodipy, 5tbuph-bodipy and phCz-4CzTPN at room temperature.

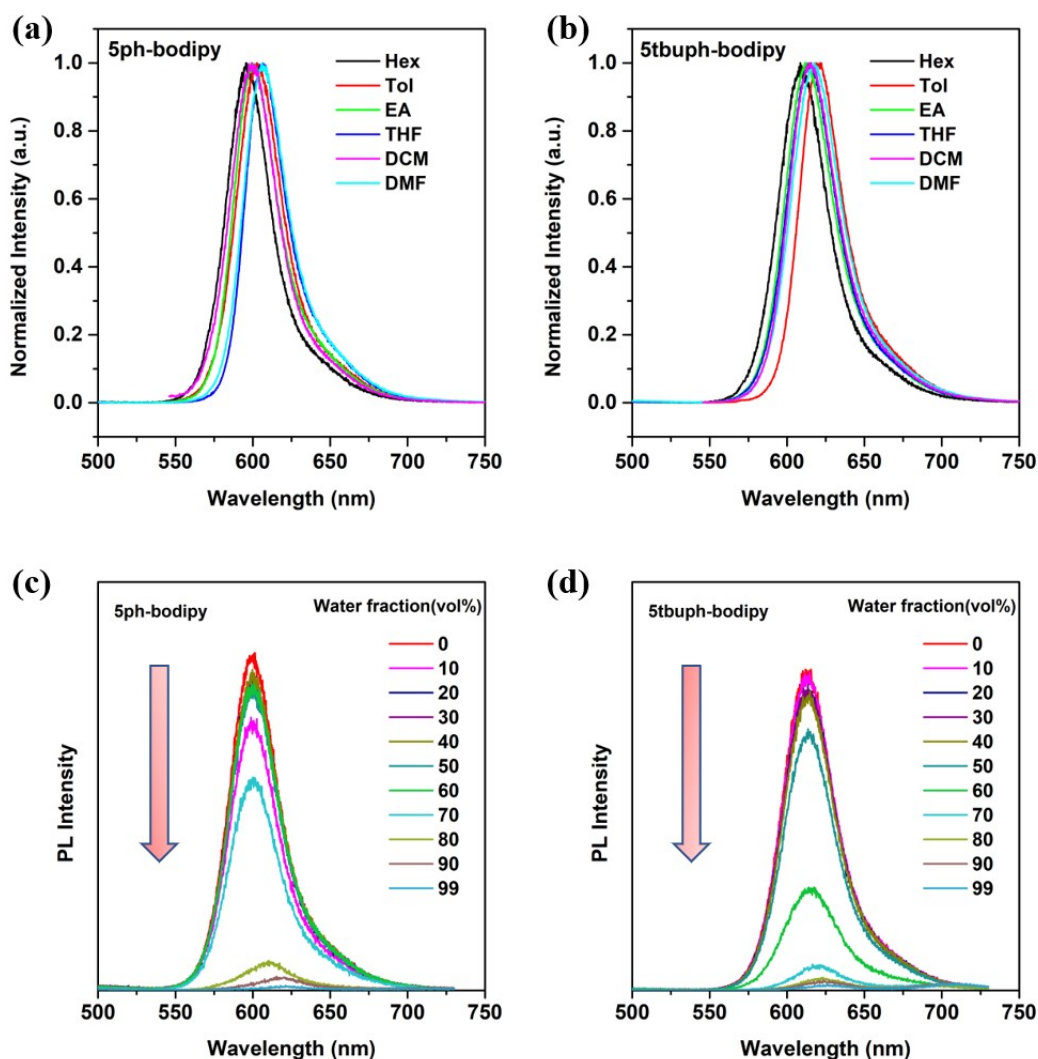


Figure S12. The normalized PL spectra of (a) 5ph-bodipy, and (b) 5tbuph-bodipy in different solvents ( $10^{-5}$  M) at 300K; the normalized PL spectra of (c) 5ph-bodipy, and (d) 5tbuph-bodipy in THF/water mixtures at different water fractions ( $10^{-5}$  M) at 300 K.

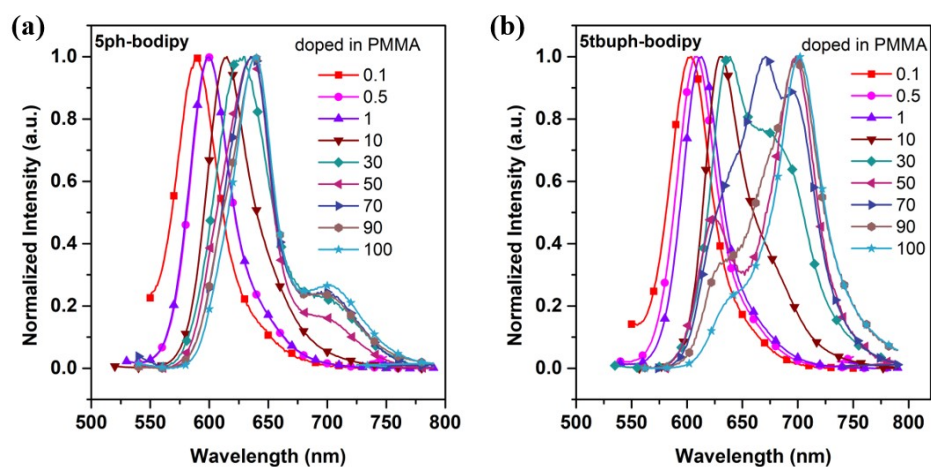


Figure S13. The normalized PL spectra of (a) 5ph-bodipy and (b) 5tbuph-bodipy doped films in PMMA matrix with various doping concentration at 300 K.

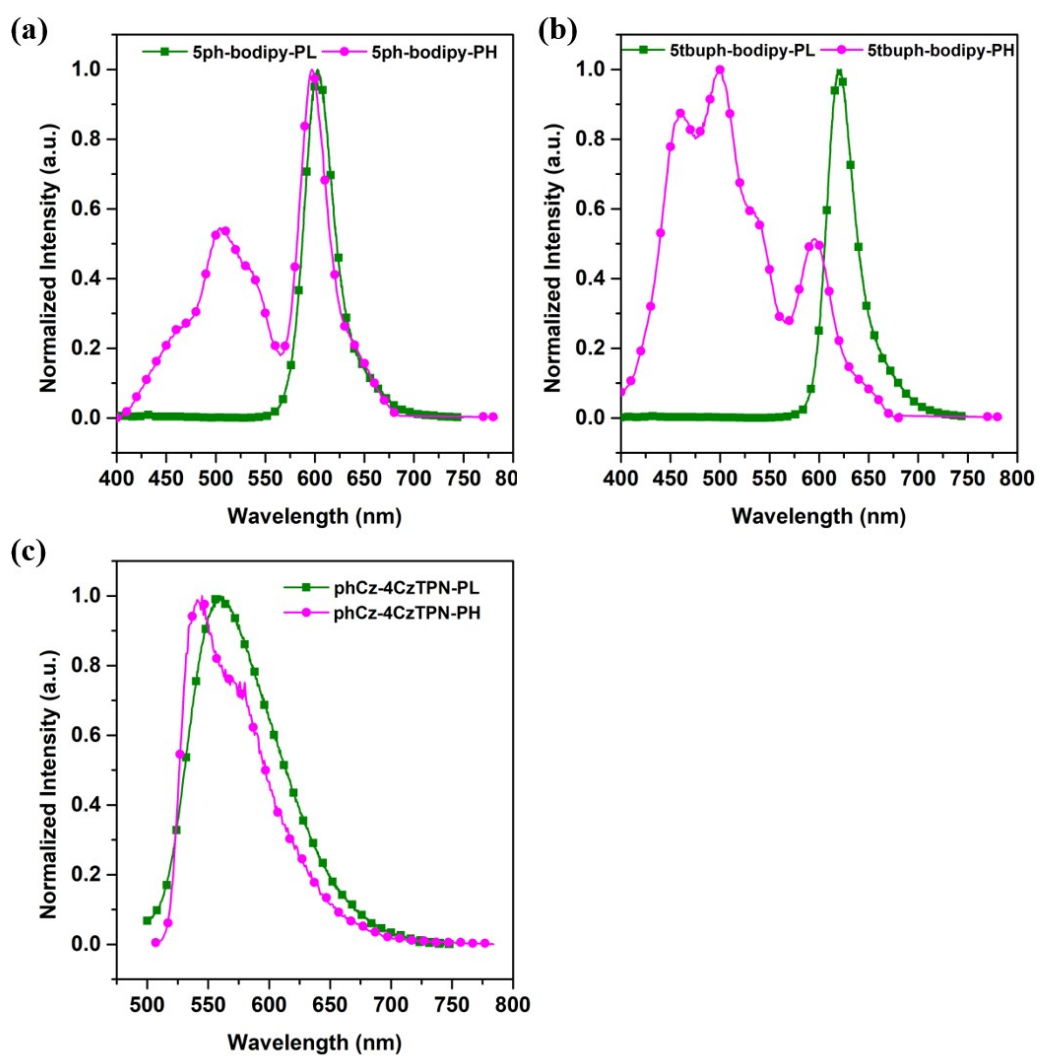


Figure S14. The normalized PL spectra and low temperature PH spectra with a delay of 100  $\mu$ s in toluene solution ( $10^{-5}$  M) at 300 K and 77 K, respectively.

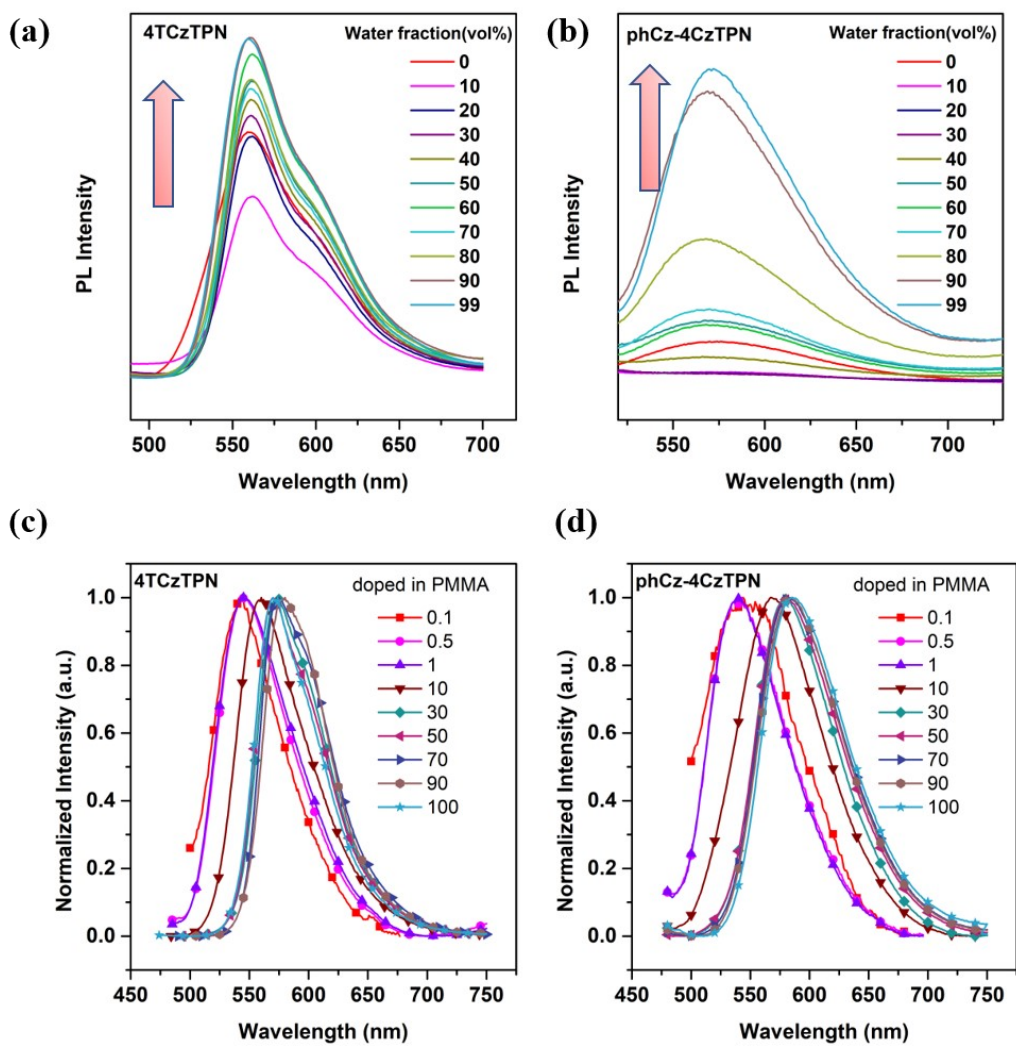


Figure S15. The PL spectra of (a) 4CzTPN, and (b) phCz-4CzTPN in THF/water mixtures at different water fractions ( $10^{-5}$  M); the normalized PL spectra of (c) 4CzTPN and (d) phCz-4CzTPN-doped films in PMMA matrix with various doping concentration at 300 K.

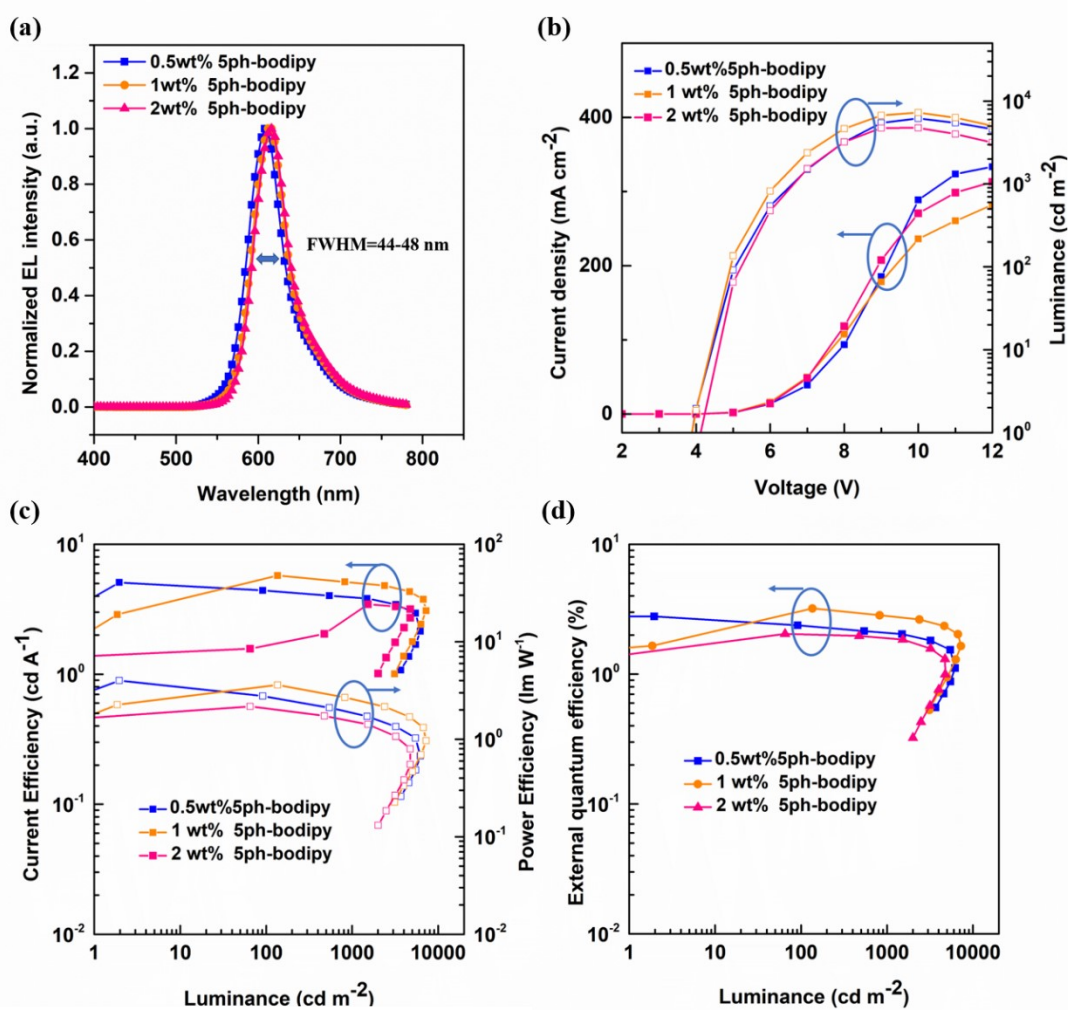


Figure S16. (a) The normalized electroluminescence (EL) spectra, (b) current density–voltage–luminance (J–V–L) characteristics, (c) current efficiencies -luminance-power efficiencies curves (CE-L-PE) and (d) external quantum efficiency-luminance (EQE-L) curves of TSF devices based on phCz-4CzTPN:5ph-bodipy.